J. Fluid Mech. (2008), *vol.* 600, *pp.* 95–104.
doi:10.1017/S0022112008000396 Printed in the United Kingdom

A many-body force decomposition with applications to flow about bluff bodies

CHIEN-C. CHANG[1,2], SHIH-HAO YANG[2,1] AND CHIN-CHOU CHU[2]

[1]Division of Mechanics, Research Center for Applied Sciences, Academia Sinica, Taipei 115, Taiwan
[2]Institute of Applied Mechanics & Taida Institute of Mathematical Sciences, National Taiwan University, Taipei 106, Taiwan
mechang@gate.sinica.edu.tw; chucc@iam.ntu.edu.tw

(Received 13 July 2007 and in revised form 3 January 2008)

The study presents a force theory for incompressible flow about several solid bodies, which enables us to examine the force contribution to each body from individual fluid elements. By employing auxiliary potential functions, we decompose hydrodynamic forces in terms of the unsteadiness of the incoming stream, vorticity within the flow, and surface vorticity on the solid bodies. The usefulness of this force decomposition is illustrated by examining separated flow about several circular cylinders. Guidelines were obtained for finding an optimal arrangement to achieve significantly small drag exerted on the cylinders.

1. Introduction

It has always been of interest to see how forces exerted on a body for flow in nature (such as bird flight) or in engineering (such as flow about an aircraft) are related to the structures of the flow (see e.g. Lighthill 1986*a*). In view of advances in numerical and measurement techniques, a theory that helps to clarify the relationship between the force and the various flow structures is useful and necessary as a large part of the flow or the entire flow field can be measured or computed. For example, if we consider a flow about a circular cylinder or sphere, the fluid meets a buffer layer in front of the body, develops a boundary layer when flowing along its shoulder, and may separate further downstream, evolving into a pair of wake vortices. Can we tell in quantity how the individual flow structures, or more precisely fluid elements, contribute to the drag exerted on the cylinder or sphere?

In the literature, there are several useful force theories which shed light on different aspects of hydrodynamic or aerodynamic forces. Circulation theory is the early attempt at predicting the lift (see e.g. Howarth 1935; Sears 1956, 1976). These authors provided insightful relationships between forces and inviscid models in terms of boundary-layer separation, vortex shedding and conservation of circulation. Subsequent studies are meant to provide exact means or theories for hydrodynamic forces through a rigorous analysis of the equation for viscous flow; see e.g. Phillips (1956), Payne (1958), Wu (1981), Quartapelle & Napolitano (1983), and in particular, Howe and colleagues (1989*a*, *b*, 1991, 1995, 2001), Kambe (1986) as well as Wells (1996) for inviscid and viscous flow. On the other hand, Lighthill (1986*b*) developed the ideas which validate a separation of hydrodynamic loadings into potential flow forces and vortex-flow forces. The applied force was deliberately explained as the rate of change of a momentum, defined by an absolutely convergent integral.

Some time ago, we proposed a diagnostic force theory to distinguish the contribution of individual fluid elements to hydrodynamic forces (Chang 1992). The theory starts from the D'Alembert theorem stating that the incompressible potential flow predicts no force exerted on a body if the incident flow is a constant uniform stream. Incompressible potential flow means that there is no single fluid element possessing non-zero vorticity or dilation. It is therefore considered that in more realistic flow, any fluid element with non-zero vorticity or dilation may be considered as a source of the hydrodynamic force. Based on this observation, we proposed to decompose the force in any given direction to consist of three components: (i) the potential force due to the body motion or the accelerating incident stream; (ii) the force due to vorticity strictly within the flow regime; (iii) the force due to the surface vorticity which can further be divided to two parts: one is the frictional force and the other called the friction-like force. Each of (ii) and (iii) is written in the form of an integral in which the integrands are appropriately called the volume and surface force elements, respectively. The volume element is rapidly decaying away from the body, and accounts for most of the force contribution for largely separated flow. The viewpoint has been applied to examine the definition of starting vortex (Chang, Hsiau & Chu 1993), the effect of suction for flow control (Chu *et al.* 1996), and extended to compressible flow to examine force contributions by various structures in the flow (Chang & Lei 1996*a*, *b*; Chang, Su & Lei 1998). Here, the force decomposition is extended to be applicable to flow about many bodies with applications to separated flow about bluff bodies. Similar formulae were derived by Ragazzo & Tabak (2007), but with different applications. In particular, we consider flow about several circular cylinders, and illustrate how the force decomposition can help to find the configuration of the cylinders to achieve significantly small total drag on the cylinder system.

2. Auxiliary potential

Let us first determine the nature of potential solution. The potential ϕ satisfies $\nabla^2\phi = 0$, and is required to vanish at infinity. The general solution at great distances r from the bodies in three dimensions is given by

$$\phi = (\boldsymbol{A}\cdot\nabla)\frac{1}{r} + \cdots = -\frac{\boldsymbol{A}\cdot\boldsymbol{n}}{r^2} + \cdots . \tag{2.1}$$

On the other hand, the potential solution at great distances r in two dimensions is given by

$$\phi = -(\boldsymbol{A}\cdot\nabla)\log r + \cdots = -\frac{\boldsymbol{A}\cdot\boldsymbol{n}}{r} + \cdots \quad . \tag{2.2}$$

In both (2.1) and (2.2), the vector $\boldsymbol{A}$ depends on the specific geometry and the motion of the solid bodies and is independent of the coordinates. The exact $\boldsymbol{A}$ requires a complete solution of the equation $\nabla^2\phi = 0$ (cf. Landau & Lifshitz 1987) and appropriate boundary conditions. The corresponding velocity $\nabla\phi$ decays as $1/r^3$ in three dimensions, and $1/r^2$ in two dimensions.

3. The force theory for N solid bodies

Consider flow past N solid bodies. The flow past a collection of solid bodies in a uniform stream is assumed to be governed by the Navier–Stokes and continuity

equations, which are given in dimensionless form,

$$\frac{\partial \boldsymbol{v}}{\partial t} + (\boldsymbol{v}\cdot\nabla\boldsymbol{v}) = -\nabla P + \frac{2}{Re}\Delta\boldsymbol{v}, \tag{3.1}$$

$$\nabla\cdot\boldsymbol{v} = 0, \tag{3.2}$$

where $\boldsymbol{v}$ denotes the velocity and P the pressure, and $Re = 2\rho Ua/\mu$ is the Reynolds number with ρ the density and μ the viscosity, U the characteristic velocity and a the characteristic length. The dimensional velocity $\boldsymbol{v}^*$, time t^* and pressure P^* are related to their dimensionless counterparts by $\boldsymbol{v}^* = U\boldsymbol{v}$, $t^* = at/U$ and $P^* = \rho U^2 P$. Also, the drag coefficient is defined by $C_D = D^*/\rho U^2 a$, and D^* is the drag. Let us now determine how fluid elements contribute to the drag force on the solid body. The uniform incident velocity is $\boldsymbol{c}(t) = c(t)\boldsymbol{i}$, The potential ϕ in the preceding section is required to satisfy $\nabla\phi\cdot\boldsymbol{n} = -\boldsymbol{i}\cdot\boldsymbol{n}$ on the ith body, and $\nabla\phi\cdot\boldsymbol{n} = 0$ on other body surfaces, where $\boldsymbol{n}$ is the normal vector pointing inward from the bodies. Let V_R be the volume of fluid enclosed by S, which consists of the body surfaces S_i, $i = 1, \ldots, N$, and a spherical surface S_R of large radius R. Taking inner products with $\nabla\phi$ on both sides of (3.1), and integrating over the entire flow region yields

$$\int_{S_i\cup S_R} P\boldsymbol{n}\cdot\nabla\phi\,\mathrm{d}A = \int_{S_R}\phi\frac{\partial\boldsymbol{v}}{\partial t}\cdot\boldsymbol{n}\,\mathrm{d}A - \int_{V_R}\boldsymbol{v}\times\omega\cdot\nabla\phi\,\mathrm{d}V + \frac{2}{Re}\int_{S_1\ldots\cup S_N}\boldsymbol{n}\times\omega\cdot\nabla\phi\,\mathrm{d}A. \tag{3.3}$$

Applying the uniform stream condition in the far field and the boundary conditions on the solid body surfaces, we can carry out the integral on the left-hand side and the first one on the right-hand side with $R\to\infty$ to obtain

$$\int_{S_i} P(\boldsymbol{i}\cdot\boldsymbol{n})\mathrm{d}A = 4\pi(\boldsymbol{A}\cdot\dot{\boldsymbol{c}}) - \int_V \boldsymbol{v}\times\omega\cdot\nabla\phi\,\mathrm{d}V + \frac{2}{Re}\int_{S_1\ldots\cup S_N}\boldsymbol{n}\times\omega\cdot\nabla\phi\,\mathrm{d}A, \tag{3.4}$$

where V denotes the entire flow region, $\boldsymbol{A}$ is the vector associated with the potential ϕ and ω is the vorticity. If the frictional force is also included, we have the drag coefficient on the **i**th body:

$$C_D = 4\pi(\boldsymbol{A}\cdot\dot{\boldsymbol{c}}) - \int_V \boldsymbol{v}\times\omega\cdot\nabla\phi\,\mathrm{d}V + \frac{2}{Re}\left(\int_{S_1\ldots\cup S_N}\boldsymbol{n}\times\omega\cdot\nabla\phi\,\mathrm{d}A + \int_{S_i}\boldsymbol{n}\times\omega\cdot\boldsymbol{i}\,\mathrm{d}A\right). \tag{3.5}$$

In brief, we write $C_D = C_{Da} + C_{Dv} + C_{Ds}$. The expression shows that the drag consists of the three contributions: the inertial force due to accelerating distant fluid, the force due to the vorticity within the flow, and the force due to surface vorticity. In (3.5), the integrand $-\boldsymbol{v}\times\omega\cdot\nabla\phi$ is called the volume drag element, and $2\boldsymbol{n}\times\omega\cdot\nabla\phi/Re$ is called the friction-like force (Chang 1992). Either of them may be termed the vortex force elements. A salient feature is: only the volume drag elements near the solid bodies contribute significantly to the drag force because $\nabla\phi$ is rapidly decaying away from the body. Also the potential function ϕ can be considered as the geometric factor of the configuration, for each flow condition for a fixed configuration can be associated with a unique ϕ.

If we consider the force in other directions, say $\boldsymbol{j}$, normal to $\boldsymbol{i}$, then ϕ has to satisfy $\nabla\phi\cdot\boldsymbol{n} = -\boldsymbol{j}\cdot\boldsymbol{n}$ on the ith body surface; $\nabla\phi\cdot\boldsymbol{n} = 0$ on other body surfaces. The force along the $\boldsymbol{j}$-direction is given by

$$C_J = -\int_V \boldsymbol{v}\times\omega\cdot\nabla\phi\,\mathrm{d}V + \frac{2}{Re}\left(\int_{S_1\ldots\cup S_N}\boldsymbol{n}\times\omega\cdot\nabla\phi\,\mathrm{d}A + \int_{S_i}\boldsymbol{n}\times\omega\cdot\boldsymbol{j}\,\mathrm{d}A\right). \tag{3.6}$$

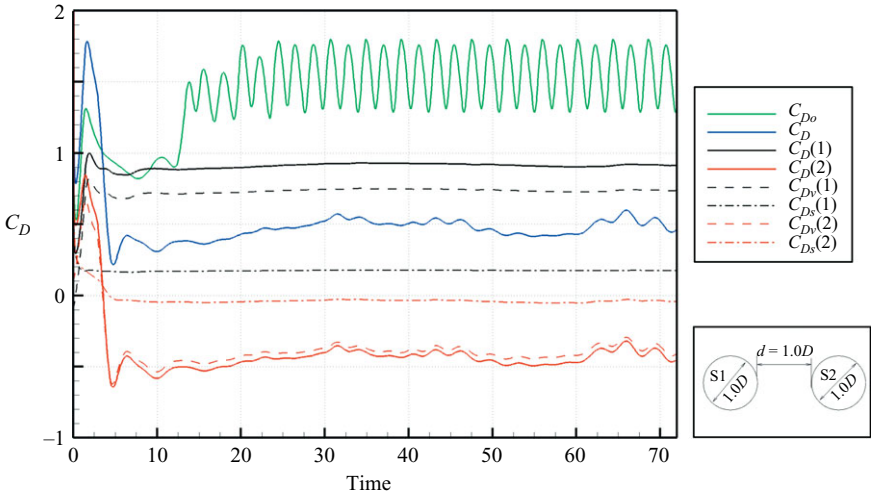

FIGURE 1. Various drag components for flow over two cylinders arranged in tandem where C_{D0} is the drag coefficient of a single cylinder.

Now if we consider the drag force on a subset of K bodies, we need an auxiliary potential ϕ that satisfies $\nabla\phi\cdot\boldsymbol{n} = -\boldsymbol{i}\cdot\boldsymbol{n}$ on $S_1\cup\cdots\cup S_K$ and $\nabla\phi\cdot\boldsymbol{n}=0$ on other body surfaces. Then the drag force on the K bodies is

$$C_D(1,\ldots,K) = 4\pi(\boldsymbol{A}\cdot\dot{\boldsymbol{c}}) - \int_V \boldsymbol{v}\times\omega\cdot\nabla\phi\,\mathrm{d}V + \frac{2}{Re}\left(\int_{S_1\ldots\cup S_N}\boldsymbol{n}\times\omega\cdot\nabla\phi\,\mathrm{d}A + \int_{S_1\ldots\cup S_K}\boldsymbol{n}\times\omega\cdot\boldsymbol{i}\,\mathrm{d}A\right). \quad (3.7)$$

Similar formulae to (3.7) have also been derived by Ragazzo & Tabak (2007).

4. Results and discussion

The present force theory will be illustrated for flow about several circular cylinders with particular emphasis on the effects of the drag elements. The complexity is increased on increasing the number of cylinders. Here, the numerical results are obtained by using the deterministic vortex method (Chang & Chern 1991) as well as the SIMPLE method of the commercial code FLUENT.

Two cylinders

Consider an impulsively started flow over two circular cylinders of diameter $D=2a$ arranged in tandem. There have been several studies on a wide range of flow conditions (Zdravkovich 1977; Kiya *et al.* 1993), but the present analysis sheds further light from a completely different viewpoint. Figure 1 shows the various force components of the drag exerted on the two cylinders at $Re=1000$. Initially, the two cylinders have little mutual interaction. The drag coefficient $C_D(1)$ for the front cylinder drops quickly, then rises to achieve a maximum at $t=1.5$, and then maintains a steady value at 0.82 from $t=2$. A further look at the drag $C_D(1)$ decomposed into the component $C_{Dv}(1)$ due to volume vorticity and $C_{Ds}(1)$ due to surface vorticity, shows that $C_{Dv}(1)$ starts from a small negative value and rises to a fairly stationary value 0.58 (on average), while $C_{Ds}(1)$ drops from a large value very quickly to 0.17. The drag coefficient $C_D(2)$ of the rear cylinder behaves similarly to $C_D(1)$ initially,

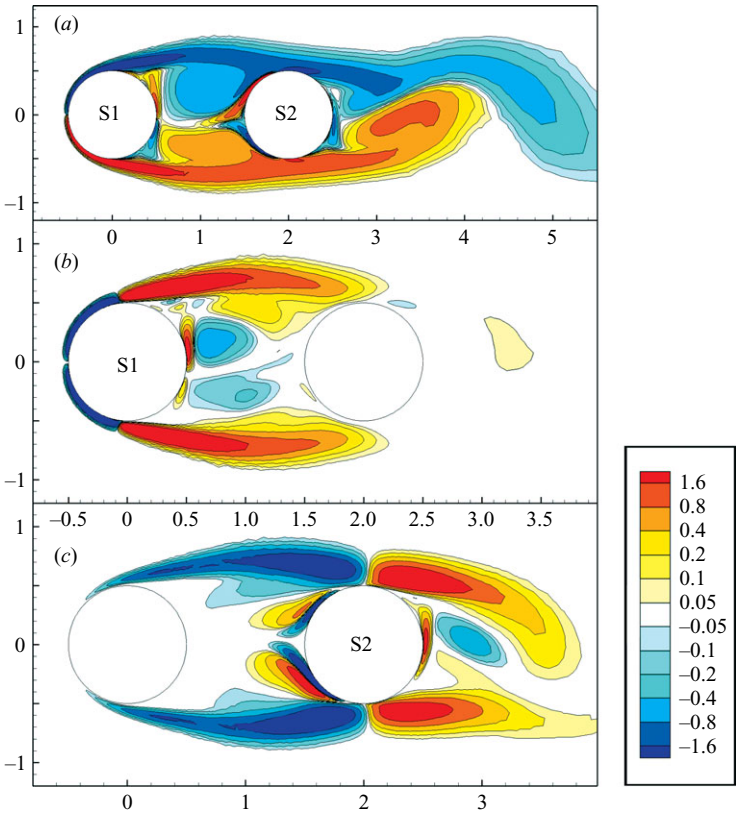

FIGURE 2. Flow field for two cylinders in tandem arrangement at $t = 36$, (*a*) vorticity contours, (*b*) volume drag elements for S1 and (*c*) volume drag elements for S2.

but decreases dramatically during the time period from $t = 1.5$ to become -0.46 (on average) after time $t = 6$. A further look at the drag $C_D(2)$ decomposed to volume drag $C_{Dv}(2)$ and surface drag $C_{Ds}(2)$, shows that $C_{Dv}(2)$ is almost identical to $C_D(2)$ after a short initial period, while $C_{Ds}(2)$ drops gradually in an initial period and becomes negligible after $t = 6$.

How do these behaviours relate directly to the flow structures in the flow? Let us sample the time instant $t = 36$, and investigate the vorticity distribution as well as the volume drag elements with respect to each cylinder (figure 2). The boundary layer in front of the front cylinder is always a source of negative drag elements. A very stable wake is observed to exist behind the front cylinder, and the zone of recirculation also provides negative drag elements to the front cylinder. At this instant, the shear layers originating from the front cylinder have extended to cover the shoulders of the rear cylinder, while the vortices behind the rear cylinder have shed in an alternating manner. It is significant to see that the wake behind the rear cylinder has a very small contribution to the front cylinder, but the shear layers originating from the front cylinder provide intense and negative volume drag elements to the rear cylinder. It is these negative elements that cause a negative value of the drag on the rear cylinder. As a result of the mutual interaction, the total drag coefficient C_D for the two-cylinder system has the average value 0.52 after an initial stage, which is significantly less than the time-averaged drag coefficient (about 1.52) for a single cylinder by 65.8%. From a systematic study of flow over two circular cylinders, we observed three important

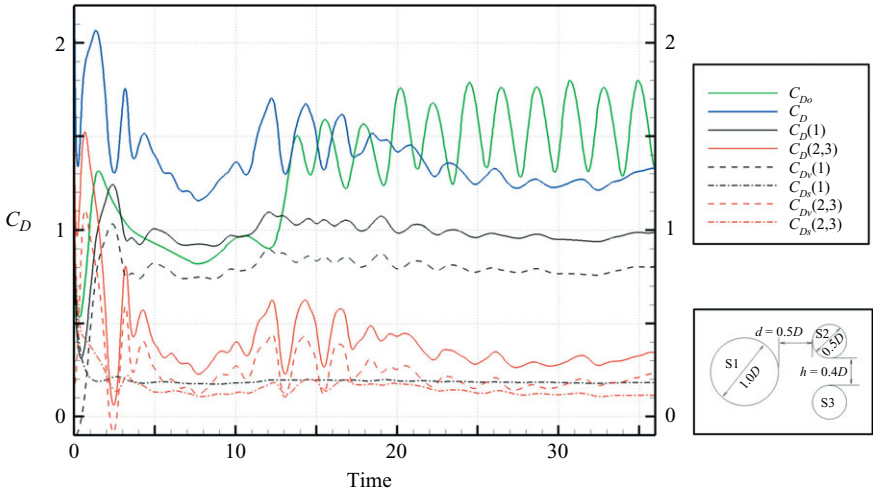

FIGURE 3. Various drag components for flow over three circular cylinders with a larger one in front and two smaller cylinders in the rear.

guidelines for achieving significantly smaller total drag for flow over several solid bodies than the sum of the drags of the flows over individual cylinders. First, the shear layers originating from the front cylinder must be separated widely enough to cover the rear cylinders. Secondly, the wake between the front cylinder and the rear cylinder must be relatively stable so that the shear layers from the front cylinder provide stable and significant negative volume drag elements to the rear cylinders. Thirdly, there is an important shielding effect so that the wake behind the rear cylinder has a relatively weak contribution to the drag of the front cylinder.

Three and four cylinders

There are many possibilities for arranging three circular cylinders in the same flow environment. According to the guidelines for flow over two circular cylinders, we consider one larger front cylinder and two smaller in-tandem cylinders a distance behind. Figure 3 shows the various force components of the drag exerted on the three cylinders. In particular, the total drag C_D is decomposed into the part exerted on the front cylinder $C_D(1)$ and the part exerted on the two rear cylinders $C_D(2, 3)$. $C_D(2, 3)$ is about three times smaller than $C_D(1)$. The average total drag coefficient for the three-cylinder system is 1.4, which is not so much less than the time-averaged drag coefficient 1.52 for flow over one single circular cylinder. Figure 4 shows the vorticity distribution as well as the volume drag elements with respect to the front cylinder as well as the two rear cylinders at $t = 36$. The most significant difference from the two-circular cylinder system is that the wake behind the front cylinder is less symmetric and allowed to shed vortices to some extent. In particular, the recirculation zone is unstable, thus reducing its contribution to drag reduction for the front cylinder. This also reduces somewhat the stability of the shear layers from the front cylinder in providing significant negative volume drag elements to the two rear cylinders.

There are two advantages in adding a fourth cylinder behind the two smaller cylinders. One is to stabilize the wake region between the front cylinder and the two middle cylinders so that the shear layers from the front cylinder are a more stable provider of negative drag elements for the two middle cylinders. The other is to delay the vortex shedding spatially (from directly behind the two middle cylinders to

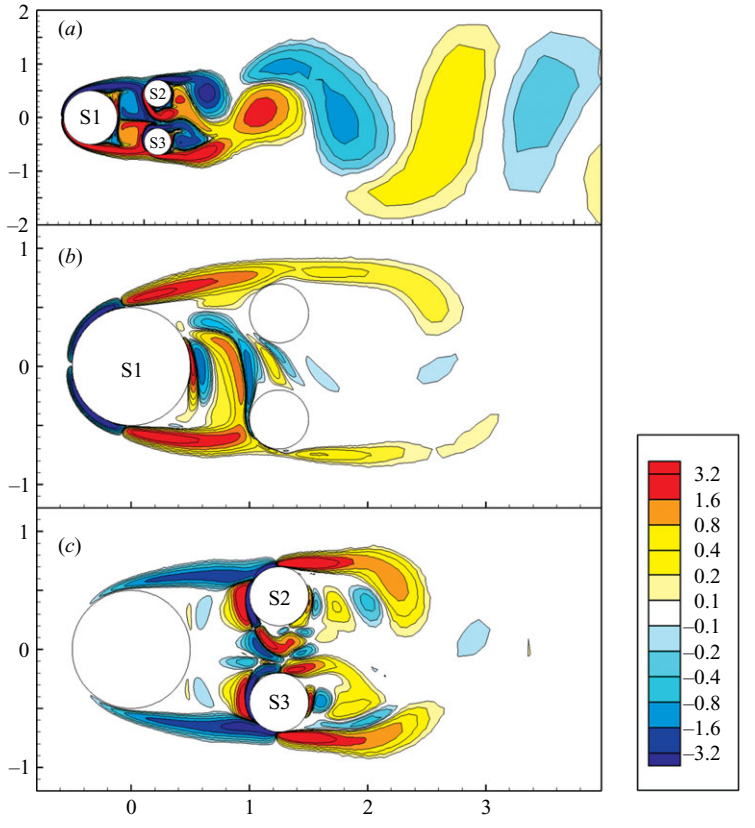

FIGURE 4. Flow field for the three-cylinder system at $t = 36$, (*a*) vorticity contours, (*b*) volume drag elements for S1, (*c*) volume drag elements for S2 + S3.

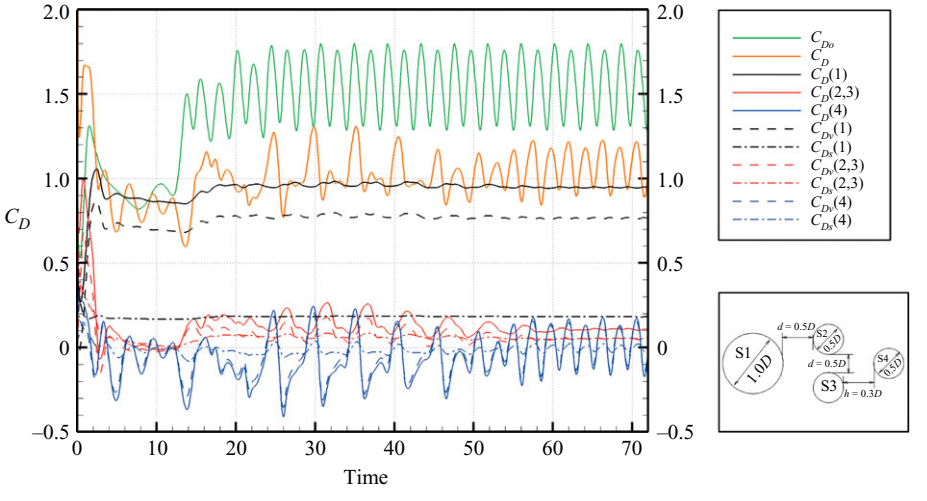

FIGURE 5. Various drag components for flow over four circular cylinders with a larger one in the front and three smaller cylinders in the rear.

behind the fourth) and the shielding effect reduces the influence from vortex shedding on the two middle cylinders. Figure 5 presents the various drag components for the four-cylinder system which shows that this is indeed the case with the drag on the

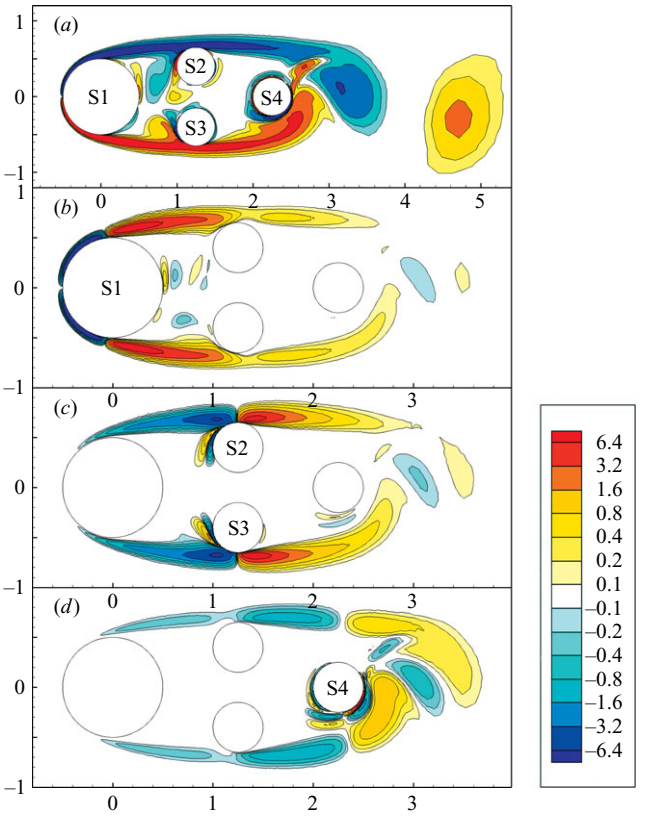

FIGURE 6. Flow field for the four-cylinder system at $t = 72$, (*a*) vorticity contours, (*b*) volume drag elements for S1, (*c*) volume drag elements for S2 + S3 and (*d*) volume drag elements for S4.

two middle cylinders $C_D(2, 3)$ further reduced (compared to the three-cylinder system) while the fourth cylinder experiences a drag $C_D(4)$ oscillating mildly with mean zero. The mutual interactions between the four cylinders are more complicated. Let us sample the time instant $t = 72$. Figure 6 shows the vorticity distribution as well as the volume drag elements with respect to the front cylinder, the two middle cylinders and the rear cylinder. It is observed that a very stable vorticity pattern is formed in the region from the front through the rear cylinders, while vortex shedding occurs in the wake behind the rear cylinder. The shielding effects are evident: the wake behind the rear cylinder has little effect on the front cylinder, and the wake right behind the front cylinder has little effect on the rear cylinder. The shear layers originating from the front cylinder and the two middle cylinders are sources of drag reduction for the rear cylinder by providing negative drag elements. The two middle cylinders receive negative drag elements from the shear layers originating from the front cylinder, and suffer from positive drag elements from their own shear layers, but little from the shedding wake behind the rear cylinder. The mutual interactions explain why the two middle cylinders are subject to very small drag, and the rear cylinder has oscillatory drag due to vortex shedding. Consequently, the four-cylinder system has experienced a total drag coefficient $C_D = 1.1$, which is even smaller than the 1.4 of the three-cylinder system.

It would be interesting to see the relative importance of individual contributions to the drag force. Tables 1 and 2 show the results for two- and four-cylinder systems,

t	$\lvert C_D(1)\rvert$	$\lvert C_{Dv}(1)\rvert$	$\lvert C_D(2)\rvert$	$\lvert C_{Dv}(2)\rvert$	$\frac{\lvert C_{Dv}(1)\rvert}{\lvert C_D(1)\rvert}(\%)$	$\frac{\lvert C_{Dv}(2)\rvert}{\lvert C_D(2)\rvert}(\%)$
2	1.48	1.29	1.57	1.37	86.8	87.5
4	1.33	1.17	1.93	1.76	88	91.2
6	1.31	1.17	1.71	1.59	89.4	93.1
12	1.17	1.04	1.48	1.37	88.7	92.6
36	1.07	0.93	1.35	1.25	87.6	92.4

TABLE 1. Volume drag ratios for two cylinders.

t	$\lvert C_D(1)\rvert$	$\lvert C_{Dv}(1)\rvert$	$\lvert C_D(2,3)\rvert$	$\lvert C_{Dv}(2,3)\rvert$	$\lvert C_D(4)\rvert$	$\lvert C_{Dv}(4)\rvert$	$\frac{\lvert C_{Dv}(1)\rvert}{\lvert C_D(1)\rvert}(\%)$	$\frac{\lvert C_{Dv}(2,3)\rvert}{\lvert C_D(2,3)\rvert}(\%)$	$\frac{\lvert C_{Dv}(4)\rvert}{\lvert C_D(4)\rvert}(\%)$
1.5	1.83	1.62	1.53	1.29	0.95	0.76	88.1	84.2	80.5
5	1.69	1.52	1.39	1.24	0.61	0.47	90.1	89	76.6
14	1.42	1.27	1.13	1.01	0.82	0.7	89.9	89.5	84.6
26	1.56	1.41	1.32	1.18	0.92	0.78	89.8	89	84.8
72	1.49	1.35	1.19	1.07	0.6	0.49	90.5	90.1	82.2

TABLE 2. Volume drag ratios for four cylinders.

from which we observed that the C_{Dv} for individual cylinders forms a large fraction of the total drag (more than 80 % or even 90 %). This provides a good basis for using the volume integrals as a diagnostic tool for analysing forces. For the present cylinder arrangements, the total lift is relatively smaller than the total drag, and oscillates about the mean zero. The oscillations come mainly from the unsymmetric wake force element distributions behind the rear cylinder.

5. Concluding remarks

In this study, we have presented a force decomposition for N bodies to analyse the force contributions to any sub-collection of these bodies by individual fluid elements (or flow structures). The usefulness of the decomposition was illustrated for flow about several circular cylinders. In particular, the present investigation yields three guidelines that are important for achieving significantly smaller total drag for flow over several circular cylinders than the sum of the drags of flow over individual cylinders. In principle, the guidelines for analysing hydrodynamic/aerodynamic forces can be applied to any flow systems supported by vortex forces such as bird flight and fish swimming. The viewpoint and method of analysis can be applied to extend our previous force theory for viscous compressible flow about single bodies to many bodies.

The work is supported in part by the National Science Council of the Republic of China under the Contract No. NSC94-2212-E-002-047 and NSC 94-2111-M-002-016.

REFERENCES

CHANG, C. C. 1992 Potential flow and forces for incompressible viscous flow. *Proc. R. Soc. Lond.* **437**, 517–525.

CHANG, C. C. & CHERN, R. L. 1991 A numerical study of flow around an impulsively started circular cylinder by a deterministic vortex method. *J. Fluid Mech.* **233**, 243–263.

Chang, C. C. & Lei, S. Y. 1996*a* On the sources of aerodynamic forces: steady flow around a sphere or a cylinder. *Proc. R. Soc. Lond.* **452**, 2369–2395.

Chang, C. C. & Lei, S. Y. 1996*b* An analysis of aerodynamic forces on a delta wing. *J. Fluid Mech.* **316**, 173–196.

Chang, C. C., Hsiau, Y. C. & Chu, C. C. 1993 Suction effect on an impulsively started circular cylinder: vortex structure and drag reduction. *Phys. Fluids* A **5**(11), 2826–2830.

Chang, C. C., Su, J. Y. & Lei, S. Y. 1998 On aerodynamic forces for viscous compressible flow. *Theor. Comput. Fluid Dyn.* (Special issue in honor of Sir James Lighthill) **10**, 71–90.

Chu, C. C., Chang, C. C., Liu, C. C. & Chang, R. L. 1996 Suction effect on an impulsively started circular cylinder: vortex structure and drag reduction. *Phys. Fluids* **8**, 2995–3007.

Howarth, L. 1935 The theoretical determination of the lift coefficient for a thin elliptic cylinder. *Proc. R. Soc. Lond.* **149**, 558–586.

Howe, M. S. 1989*a* On unsteady surface forces, and sound produced by the normal chopping of a rectilinear vortex. *J. Fluid Mech.* **206**, 131–153.

Howe, M. S. 1989*b* Structural and acoustic noise generated by a large-eddy breakup device. *Proc. R. Soc. Lond.* A**424**, 461–486.

Howe, M. S. 1991 On the estimation of the sound produced by complex fluid–structure interactions, with applications to a vortex interacting with a shrouded rotor in a duct. *Proc. R. Soc. Lond.* **433**, 573–598.

Howe, M. S. 1995 On the force and moment on a body in an incompressible fluid, with application to rigid bodies and bubbles at high and low Reynolds numbers. *Q. Mech. Appl. Maths.* **48**, 401–426.

Howe, M. S., Lauchle, G. C. & Wang, J. 2001 Aerodynamic lift and drag fluctuations of a sphere. *J. Fluid Mech.* **436**, 41–57.

Kambe, T. 1986 Acoustic emissions by vortex motions. *J. Fluid Mech.* **173**, 643–666.

Kiya, M., Mochizuki, O., Ido, Y., Suzuki, T. & Arai, T. 1993 Flip-flopping flow around two bluff bodies in tandem arrangement. *Bluff-body Wakes, Dynamics and Instabilities*. Springer.

Landau, L. D. & Lifshitz, E. M. 1987 *Fluid Mechanics*, 2nd edn. Pergamon.

Lighthill, M. J. 1986*a* *An Informal Introduction to Theoretical Fluid Mechanics*. Clarendon.

Lighthill, M. J. 1986*b* Fundamentals concerning wave loading on offshore structures. *J. Fluid Mech.* **173**, 667–681.

Payne, R. B. 1958 Calculations of unsteady flow past a circular cylinder. *J. Fluid Mech.* **3**, 81–86.

Phillips, O. M. 1956 The intensity of aeolian tones. *J. Fluid Mech.* **1**, 607–624.

Quartapelle, L. & Napolitano, M. 1983 Force and moment in incompressible flows. *AIAA J.* **22**, 1713–1718.

Ragazzo, C. G. & Tabak, E. G. 2007 On the force and torque on systems of rigid bodies: a remark on an integral formula due to Howe. *Phys. Fluids* **19**, 057108.

Sears, W. R. 1956 Some recent developments in airfoil theory. *J. Aeronaut. Sci.* **23**, 490–499.

Sears, W. R. 1976 Unsteady motion of airfoil with boundary layer separation. *AIAA J.* **14**, 216–220.

Wells, J. C. 1996 A geometrical interpretation of force on a translating body in rotational flow. *Phys. Fluids* **8**, 442–450.

Wu, J. C. 1981 Theory for aerodynamic force and moment in viscous flows. *AIAA J.* **19**, 432–441.

Zdravkovich, M. M. 1977 Review of flow interference between two circular cylinders in various arrangements. *Trans. ASME I: J. Fluids Engng* **99**, 618–633.